# Locally Adaptive Topology Preservation for Diffeomorphic Registration in Medical Imaging

WEI LIU[1] LEI-TING CHEN[1] YUN-JIN CHEN [2]
GUO-CHENG YANG [1] HONG-BIN CAI[1]
[1]School of Computer Science and Engineering, University of Electronic Science and Technology of China, Chengdu, CHINA
[2]National Laboratory for Parallel and Distribution Processing, National University of Defense Technology, Changsha, CHINA
WeiLiu0405@gmail.com

*Abstract:* Diffeomorphic registration has become an active research field presently in medical image registration because of its the differential transformation with invertibility between anatomic individuals. In this paper, we propose a novel method named Locally Adaptive Topology Preservation for Diffeomorphic Registration, which is able to obtain accurate approximation for the local tangent space on the Lie group manifold and yield more plausible diffeomorphisms for spatial transformations. In order to incarnate the local geometric structure of the Lie group, the local linear approximation is adaptively optimized by selecting appropriate neighborhoods for each sample point. Furthermore, we investigate the Lie group structure of the Symmetric Positive Definite (SPD) matrices and evaluate the effectiveness of the algorithm by utilizing several sets of brain images. Experimental results demonstrate that our algorithm has a higher degree of topology preservation on a dense high-dimensional deformation field and performs better in the noisy setting.

*Key–Words:* Diffeomorphic registration, Lie group, Neighborhood selection, Symmetric positive definite matrices, Medical images

## 1 Introduction

In medical image registration, estimating a highly non-linear deformation corresponding to anatomic variability between individuals is a challenging research field [1, 2]. A basic assumption of this task is that two individuals have the same anatomic structures, and the transformation has smoothness and topological properties. In nature, topology preservation is a global constraint to maintain connectivity between local neighbor anatomic structures. Without any strict constraint, the continuity and invertibility of a transformation is not necessarily guaranteed.

There has been a considerable body of previous research done on preserving topology for non-rigid image registration. A general approach to implement topology preservation is to impose positivity constraint on the Jacobian of the transformation.

Musse $et\ al$ [3] described a spline-based topology preserving image registration. By utilizing a continuous hierarchical structure, they controlled topological constraints to enforce Jacobian positivity over the continuous domain, not only on the discrete grid. However, it only works on two dimensional deformation field. Vincent Noblet $et\ al$ [4] extended the work of [3] to three dimensional registration. In order to yield constraints on optimization, they employed the blockwise descent algorithm. Rohlfing $et\ al$ [5] penalized deviations of the Jacobian determinant of the deformation to obtain a local volume-preservation constrain. Christensen $et\ al$ [6, 7] addressed the framework of elastic solids and viscous fluids, which constrained the transformation to be positive definite Jacobian via partial differential equations. Bilge $et\ al$ [8] used deformation gradients to approximate the displacement field Jacobian and imposed topology preserving regularity on a irregular deformation field. Ashburner $et\ al$ [9] divided the domain into a triangular mesh where Jacobian of the triangle relies on the rate of change prior potential. Haber $et\ al$ [10] introduced discretization on a triangulation to prevent twists and singular Jacobian. They controlled the determinant of the Jacobian by using inequality constraints.

In recent years, a diffeomorphic model has been developed for medical image registration [11, 12, 13]. A diffeomorphism is a one-to-one mapping between individuals with smooth and invertible properties, which can perform the biologically reasonable deformation while avoiding the physically implausible phenomena. In contrast to non-diffeomorphic registration in medical images, diffeomorphic methods guarantee a smooth and invertible correspondence over the whole domain. In [11], Marsland $et\ al$ represented diffeomorphic warp as a time varying velocity field, which is formulated with geodesic interpolating spline base, and then approximated the diffeomorphism by using iterative greedy algorithm. In [13], Arsigny $et\ al$ proposed the Log-Euclidean framework,in which Euclidean operations are performed via logarithms, while having inversion-invariant property. They efficiently take advantage of stationary vector fileds to parameterize diffeomorphisms. Vercauteren $et\ al$ [14] represented diffeomorphic transformation as a stationary velocity field, the space of which can form a Lie group under composition operation in the Log-Euclidean framework. Diffeomorphisms should have been continuous so as to enforce consistency under compositions of the deformations. However, the composed transformation is computed on discrete grid. Therefore, the Jacobian is not necessary to be positive. In [12], Ashburner used diffeomorphic deformation as a constant time flow of vector fields. Within a discrete time, large-deformation diffeomorphisms can be dealt with by a composition of a series of small deformations.

However, there are two limitations on methods above. 1) These methods do not consider the underlying nonlinear structure of data on high-dimensional diffeomorphisms space. However, the high-dimensional data contains more structural information. 2) They also ignore noise in images. A topology preserving displacement field from a noisy observation does not necessarily preserve topology.

In this paper, we propose a diffeomorphic registration method, called locally adaptive topology preservation for diffeomorphic registration in medical imaging. The proposed method builds on the learning method presented in [16] and the original diffeomorphic demons algorithm [14]. During registration, we apply symmetric positive definite (SPD) matrices, which could form a Lie group. In the context of Lie group, Jacobian matrix at the identity element ($Id$) corresponds to the tangent space vector. The tangent space is constructed from a neighborhood of the identity element. The neighborhood is closely related to the curvature. Due to the highly-varying curvature of the manifold and noise, it is usually difficult to build a linear approximation of the nonlinear local tangent space. So far, little work has been done on studying the influence from the size of the neighborhood. As mentioned in [15], the exponential is a diffeomorphism between a neighborhood of the zero in the Lie algebra and a neighborhood of the identity element in the Lie group, but it remains obscure what size the neighborhood is. Therefore, the information of neighborhood needs to be accurately estimated to monitor deformation fields. In the literatures, there are two commonly used strategies for selecting the neighborhoods: K-NN [17] and $\epsilon$-N [18].

The contribution of our work is that we make use of variant neighborhood selections to estimate the local tangent space with higher accuracy, and then, we are able to achieve a higher degree of topology preservation on a dense high-dimensional deformation field. As a by-product, using PCA in constructing the tangent space processing reduces the noise.

The remainder of the paper is organized as follows: In section 2, we overview some related knowledge about Lie group and Lie algebra. In section 3 describes how to take advantage of adaptive neighborhood selection to approximate to tangent space, then to achieve topology preservation. Our proposed algorithm is presented in detail. In section 4, we demonstrate the experiment results on MR images and evaluate our method. Section 5 concludes the work with discussions.

## 2 Preliminaries

### 2.1 Matrix Lie Group And Lie Algebra

We consider a Matrix Lie group as a feature space in this paper. A Lie group $GL(m)$ is an abstract group with a differential manifold on which the operations of group multiplication and inversion are smooth diffeomorphisms [19].

Due to the fact that a nonlinear manifold is a topological space, a Lie group lacks a vector space structure. A tangent space $T_\varepsilon G$ at a given point on the manifold is a vector space. The tangent space contains all tangent vectors at this point. Therefore, a common application in dealing with the nonlinearity is locally homeomorphic to Euclidean space. It takes advantage of the projection to a tangent space at the point to approximate the manifold. The tangent space at the identity element on the Lie group is identified with the Lie algebra $gl(m)$. Definitions and notation:

- $GL(m)$ represents a group of real invertible $m \times m$ matrix
- $gl(m)$ represents a linear vector space of $m \times m$ matrices
- $exp$ denotes the exponential map
- $log$ denotes the logarithm

Between the finite dimensional Lie group and the Lie algebra, the group exponential maps elements of Lie algebra to the corresponding elements in the Lie group. The inverse of the exponential is the logarithm,

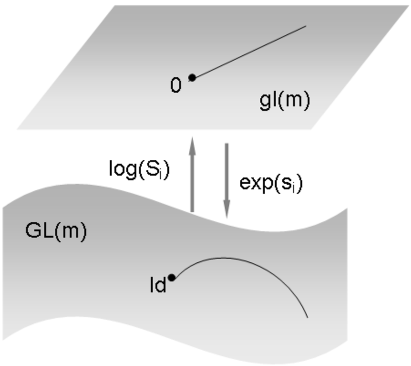


Figure 1: Maps between Lie group and Lie algebra: The differential mapping of the exponential at the zero is the $Id$, the tangent space at the $Id$ is the Lie algebra of the group

it maps elements in the Lie group to elements of the Lie algebra, see Fig.1.

$$S_i = exp(s_i), \qquad s_i = log(S_i), \tag{1}$$

where $S_i \in GL(m), s_i \in gl(m)$ are elements of Lie group and Lie algebra. Since the differential of $exp$ is nowhere singular [20], $exp$ and its inverse $log$ are both diffeomorphisms. The differential of $exp$ at the zero has invertibility derived from continuity in a neighborhood of the zero due to the identity element.

If a Lie group is a matrix group, it corresponds to the algebraic matrix exponential and the matrix logarithm. The identity element is the identity matrix. The exponential and logarithm in matrix sense are given by

$$\begin{aligned} exp(s_i) &= \sum_{k=0}^{\infty} \frac{1}{i!} s_i^k, \\ log(S_i) &= \sum_{k=1}^{\infty} \frac{(-1)^{k-1}}{k} (S_i - I)^k. \end{aligned} \tag{2}$$

### 2.2 SPD Matrices On Lie Group

SPD matrices are a type of important nonlinear manifolds containing more structural information for the image registration. There are varied forms of SPD matrices, for instance, covariance region descriptors [21] and structure tensors [22].

We denote $Sym^+(m)$ as the space of SPD $m \times m$ matrices. For any SPD matrix, there exists a symmetric logarithm. Let $S_i, S_j \in Sym^+(m)$, the logarithmic product is defined as

$$S_i \odot S_j := exp(log(S_i) + log(S_j)), \tag{3}$$

where $exp(.)$ and $log(.)$ denote the matrix exponential and logarithm operators, respectively.

The group inverse of an SPD matrix is given by

$$\begin{aligned} &log(S_j^{-1}) := -log(S_j), \\ &S_i \odot S_j^{-1} := exp(log(S_i) - log(S_j)). \end{aligned} \tag{4}$$

The logarithmic multiplication $\odot$ on $Sym^+(m)$ is compatible with its structure of smooth manifold. $(S_i, S_j) \mapsto S_i \odot S_j^{-1}$ is $C^\infty$ [20]. Therefore, under logarithmic multiplication $\odot$, SPD matrices is a Lie group structure. $Sym^+(m)$ is diffeomorphic to its tangent space at the identity element. SPD matrices is mapped to the tangent space at the identity matrix. The tangent space at the identity element is identified with the Lie algebra $gl(m)$.

## 3 Methodology

### 3.1 Topology Preservation On Diffeomorphic Demons

Naturally, image registration finds an optimal spatial transformation that maps each point in the floating image to a point in the reference image, topology preservation ensures that each point in the floating image has one and only one corresponding point in the reference image so that the deformation field is diffeomorphic, otherwise, the topology is not necessarily preserved.

Our registration algorithm is built on Diffeomorphic Demons method in which transformations are assumed to belong to a group of diffeomorphisms. Given a reference image $I_r$ and a floating image $I_f$, let $S$ be a data set $[S_1, S_2, \cdots, S_n] \subset I_r, S_i \in Sym^+(m)$. For each point $S_i$, there is a k-nearest neighbourhood $E_i = [S_{i_1}, S_{i_2}, \cdots, S_{i_k}]$, $S_{i_j} \in Sym^+(m)$. Diffeomorphic Demons registration is formulated as minimizing a cost function which contains a similarity term and a regularization term, and enforces a Jacobian to add an additional regularization as a constraint. The cost function is given by

$$minE(u) = Sim(I_r, I_f \circ \varphi) + Reg(\varphi), \tag{5}$$

where Sim(.) and Reg(.) denote a similarity term and a regularization term, respectively. Diffeomorphic formulation is based on velocity flow $\phi(S_i, t), t \in [0, 1]$. Eq.(5) seeks an optimal transformation $\varphi(S_i) = \phi(S_i, t)$, $u$ is a time-dependent velocity field $u(\phi(S_i, t), t)$, $\phi$ can be obtained by the ordinary differential equation with respect to $u$,

$$\frac{d\phi(S_i, t)}{dt} = u(\phi(S_i, t), t), \phi(S_i, 0) = S_i. \tag{6}$$

For any $S_{i_j}$, there exists $u \in gl(m)$ so that the group transformation $\varphi \in GL(m)$ can be obtained by finite composition of the group exponential map $exp(u)$ at time $t = 1$, $\phi(S_i, 1) = exp(u(s_i))$. The diffeomorphic transformations are represented as the composition of

$$S_{i_j} = S_i \circ \phi = S_i \circ exp(u). \tag{7}$$

In order to establish diffeomorphism between the neighborhood of zero in the Lie algebra and the neighborhood of the identity element in the Lie group with $exp(u(0)) = Id$, the exponential map is restricted to a neighbourhood of the origin in the Lie algebra so that this correspondence is unique. As a result, the topology is preserved between Lie groups.

Furthermore, the Taylor expansion of $\varphi$ takes the form,

$$\varphi(S_i \circ exp(u)) = \varphi(S_i) + J^{\varphi}_{S_i}.u + O(\| u \|^2). \tag{8}$$

Jacobian matrix describes the derivatives of the deformations, it can be represented as follows,

$$[J^{\varphi}_{S_i}]_i = \frac{\partial}{\partial u^i}\varphi(S_i \circ exp(u)). \tag{9}$$

Let $T = [\tau_1, \tau_2, \cdots, \tau_d] \in T_\varepsilon G$ be the orthonormal basis matrix in the identity tangent space of the Lie group, $\tau_i \in R^m$. A tangent vector field (deformation field) $u$ with respect to a local coordinate chart around a point $S_i$ can be denoted by

$$u = \sum_{i=1}^{d} u^i \tau_i, \tag{10}$$

where $u^i$ is the component of $u$ in a given coordinate system. Combining Eq.(9) and (10), we may re-write the Jacobian matrices as follows,

$$[J^{\varphi}_{S_i}]_i = \frac{\partial}{\partial u^i}\varphi(S_i \circ exp(\sum_{i=1}^{d} u^i \tau_i)). \tag{11}$$

Jacobian matrices encode the local transformation of the deformation field, the determinant of the Jacobian is used as a strict and strong constraint for minimizing the cost function, see Eq.(5). The topology preservation on a deformation field is associated with a positive Jacobian [23]. Eq.(11) should satisfy $[J^{\varphi}_{S_i}]_i > 0$ at any point at every iteration. Negative determinants indicate that the invertibility on the space of diffeomorphisms fails. As shown in Eq.(11), Jacobian of the deformation at arbitrary point $S_i$ is computed by the orthonormal basis matrix $T_i$ of the tangent space at the identity element, the tangent space is influenced by the neighborhood of the identity element. Therefore, selecting the neighbors of the identity element is necessary to estimate an accurate approximation of the local tangent space, and finally find an accurate orthonormal basis matrix. However, due to varied curvature of the nonlinear manifold, the set of points in the neighbor is not accurately close to the tangent space. According to [24], smaller curvature near the identity element should give rise to a larger neighborhood, while larger curvature should tend to shrink the neighborhood, as a consequence, the neighborhood is closely related to the structure of data.

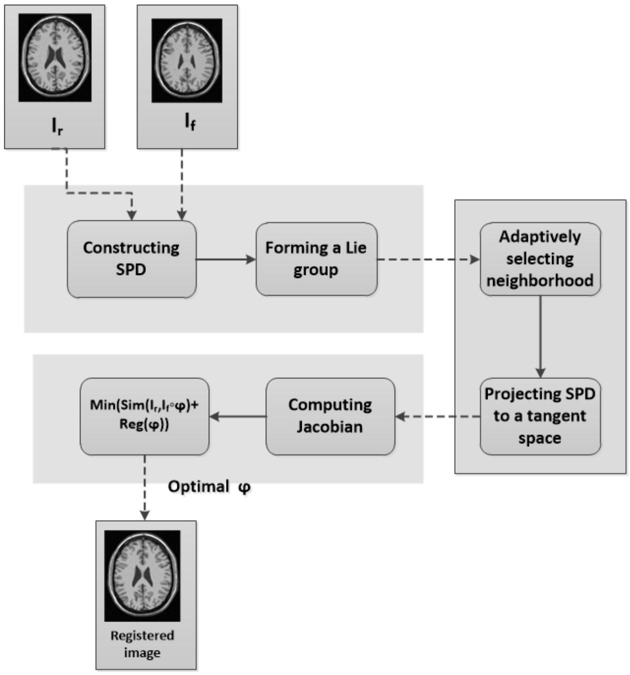


Figure 2: A flowchart of the proposed registration model using adaptive neighborhood selection method

## 3.2 Locally Adaptive Tangent Space Approximation

A Lie group is a manifold. Motivated by the idea of adaptive manifold learning [16], we introduce approximation to the tangent space at the $Id$ based on adaptive selection of the neighborhood sizes. For simplicity, the $Id$ is referred to as $\varepsilon$ in the following sections. Let $E_\varepsilon$ be a neighborhood of the $Id$, it consists of $k$ nearest neighbors $[\varepsilon_1, \varepsilon_2, \cdots, \varepsilon_k]$, $\varepsilon_j \in Sym^+(m), j = 1, 2, \cdots, k$. An optimal linear fitting to the $Id$ in the neighborhood can be established as

$$\sum_{j=1}^{k} \|\varepsilon_j - (\bar{\varepsilon} + T\theta_j\| = \|E_\varepsilon - (\bar{\varepsilon}e^{\mathrm{T}} + T\Theta\|, \tag{12}$$

where $\theta_j$ is the projection of $\varepsilon_j$ in a local neighborhood on the local PCA, $E_\varepsilon$ is the matrix of $\varepsilon_j$s. $T$ represents an orthonormal basis matrix of tangent space, $\bar{\varepsilon}$ is the mean of all $\varepsilon_j$

$$\theta_j = T^{\mathrm{T}}(\varepsilon_j - \bar{\varepsilon}) \quad j = 1...k. \tag{13}$$

$\Theta \in R^{d\times k}$ is the matrix made of $\theta_j$, also is the local coordinate corresponding to the basis $T$,

$$\Theta = [\theta_1, \theta_2, \cdots, \theta_k] = T^{\mathrm{T}}(E_\varepsilon - \bar{\varepsilon}e^{\mathrm{T}}). \tag{14}$$

By using singular value decomposition (SVD) to $E_\varepsilon - \bar{\varepsilon}e^{\mathrm{T}}$, we obtain $\sigma_1 \geq \cdots \geq \sigma_d \geq \cdots \sigma_k$, the solution of Eq.(14) is

$$\Theta = diag(\sigma_1, \sigma_2, \cdots, \sigma_d)V^{\mathrm{T}}, \tag{15}$$

where $V^{\mathrm{T}}$ represents a matrix consisting of d right singular vectors of $E_\varepsilon - \bar{\varepsilon}e^{\mathrm{T}}$ corresponding to d largest singular values, and we get $T \in R^{m\times d}$, which is the matrix formed by left singular vectors, we have

$$\|\Theta\| = \sqrt{\sum_{j\leq d}(\sigma_j)^2}, \tag{16}$$

$$\|E_\varepsilon - (\bar{\varepsilon}e^{\mathrm{T}} + T\Theta\| = \sqrt{\sum_{j>d}(\sigma_j)^2}. \tag{17}$$

According to Eq.(16) and (17), a ratio $r$ is formed as follows,

$$r = \sqrt{\sum_{j\leq d}(\sigma_j)^2 / \sum_{j>d}(\sigma_j)^2}. \tag{18}$$

This ratio is a criterion to adaptively select neighborhood.

### 3.3 Proposed Algorithm

A flowchart of the proposed registration model can be seen in Fig.2. Further details of the algorithm are described in Alg.1.

**Algorithm 1** Locally Adaptive Topology Preservation for Diffeomorphic Registration in Medical Imaging

**Input:** $I_r$ (Reference image) and $I_f$ (Floating image)
**Output:** Registered image
1: Convert $I_r$ and $I_f$ to SPD matrices;
2: Choose a minimum $k_{mim}$, a maximum $k_{maz}$ and an initial size of neighborhood $k$ for $Id$;
3: Calculate $\sigma_j$ of $E_\varepsilon - \bar{\varepsilon}e^{\mathrm{T}}$ using SVD;
4: Calculate the ratio $r$;
5: **if** $r < \eta$ (a hypothetical threshold) **then**
6: $\quad E_\varepsilon \longleftarrow E_\varepsilon^{(k)}$
7: $\quad$ go to line 30
8: **else**
9: $\quad$ **if** $k > k_{min}$ **then**
10: $\quad\quad$ delete the last column of $E_\varepsilon^{(k)}$
11: $\quad\quad E_\varepsilon^{(k)} \longleftarrow E_\varepsilon^{(k-1)}$
12: $\quad\quad k \longleftarrow k - 1$
13: $\quad\quad$ return to line 3
14: $\quad$ **end if**
15: $\quad$ **for** $k = k_{min}, \cdots, k_{max}$ **do**
16: $\quad\quad$ Find $k$ corresponding to the minimum $r^{(k)}$
17: $\quad\quad E_\varepsilon \longleftarrow E_\varepsilon^{(k)}$
18: $\quad$ **end for**
19: $\quad$ Compute $\bar{\varepsilon} + T\Theta_j$ to $E_\varepsilon$
20: $\quad$ **for** $j = k+1, \cdots, k_{max}$ **do**
21: $\quad\quad$ Compute $\theta_j = T^{\mathrm{T}}(\varepsilon - \bar{\varepsilon})$ for all $\varepsilon_j$ out of $E_\varepsilon$
22: $\quad\quad$ **if** $\|\varepsilon_j - \bar{\varepsilon} - T\theta_j\| \leq \eta\|\theta_j\|$ **then**
23: $\quad\quad\quad$ Add $\varepsilon_j$ to $E_\varepsilon$
24: $\quad\quad\quad E_\varepsilon^{(k)} \longleftarrow E_\varepsilon^{(k+1)}$
25: $\quad\quad\quad k \longleftarrow k + 1$
26: $\quad\quad$ **end if**
27: $\quad$ **end for**
28: **end if**
29: Compute the orthonormal basis $T = [\tau_1, \tau_2, \cdots, \tau_d]$ in the identity tangent space $T_\varepsilon G$
30: Compute the Jacobian at an arbitrary point
31: Minimize the cost function

## 4 Experiments

We evaluate our algorithm by comparing it with the original Diffeomorphic Demons. For convenience, Diff Demons is short for Diffeomorphic Demons in the following sections.

### 4.1 Construcing SPD Matrices

In this section, we introduce how to construct the SPD matrices. Constructing the $m \times m$ SPD matrix image feature in each pixel position is a crucial step to our algorithm. First, we extract the 128-dimensional dense-SIFT descriptors,pixel locations(x, y), the intensity I(x, y), the norm of the first derivatives of the intensities with respect to x and y. Each pixel of the image is converted to a 133-dimensional feature vector $f_i$, it is represented as follows,

$$f_i = [SIFT \quad x \quad y \quad I(x,y) \quad |\frac{\partial(x,y)}{\partial x}| \quad |\frac{\partial(x,y)}{\partial y}|]^{\mathrm{T}}. \tag{19}$$

Second, according to [25], we compute the outer products of local descriptors $f_i$ and its transpose $f_i^{\mathrm{T}}$, get a SPD matrix $S_i$

$$S_i = f_i \cdot f_i^{\mathrm{T}}, \tag{20}$$

where the size of $S_i \in Sym^+(m)$ is $133 \times 133, m = 133$. Finally, we construct a graph with a node for each point on the Lie group manifold, and with edges connecting neighboring nodes. Therefore, the neighborhood can be defined with an adaptive neighborhood around each point. Here each point is a SPD matrix. In order to reduce the influence of noise and the computation complexity, we transform a high-dimensional Lie group into a dimension-reduced one with [26] method. The dimension of $S_i \in Sym^+(m)$ is selected in the set $m = \{133, 123, 113\}$

## 4.2 Evaluation Criterion

To evaluate registration performance, we consider two criterions: error $(\%)$ and the degree of topology preservation $d_{TP}$. A topology preservation deformation field must satisfy that the Jacobian determinant is positive at any point. In order to evaluate clinical results, we use the root mean squared (RMS) error. In practice, the Jacobian is computed by finite difference on the discrete grid in stead of continuous spatial transformations, discretization leads up to the fact that Jacobians is not always positive. Therefore we use $d_{TP}$ to describe the degree of topology preservation.

$$d_{TP} = \frac{n}{N}, \tag{21}$$

where $n$ and $N$ denote the total number of points in $GL(m)$ and the number of points whose Jacobian are positive, respectively.

## 4.3 Comparison Results And Analysis

In this section, simulation results are performed on shape C, synthetic and clinical data.

### 4.3.1 Square To Shape C

Fig.3 illustrate the comparison results on transformations of a square and a shape C, as shown in (a) and (e). In this experiment, three transformations are generated for different size of neighborhood $k$ and different dimension $m$. In the case of (b) and (f), there exist folding and overlapping. In the case of (c) and (g), it indicates smoother deformation field than (b) and (d), but it is not exact enough in contrast to (d). Smoothness between two transformations need not be topology preserving, especially in medical image analysis, for example, some lesion in tissue often happens [8].

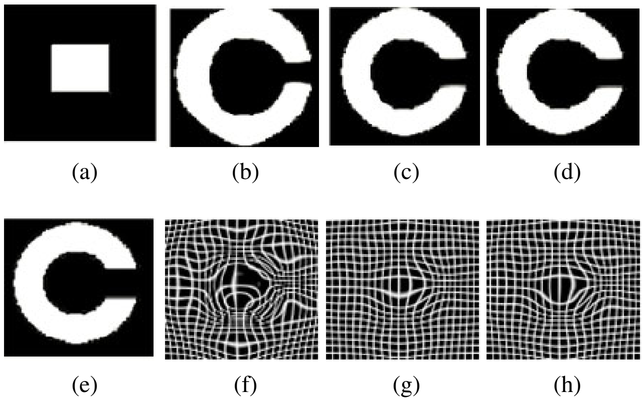


Figure 3: C experiment: (a) floating image.(e) reference image. (b) deformed result with $k = 180, m = 133$. (c) deformed result with $k = 110, m = 123$. (d) deformed result with $k = 140, m = 113$. (f)-(h) deformed fields corresponding to (b)-(d)

### 4.3.2 Synthetic Data

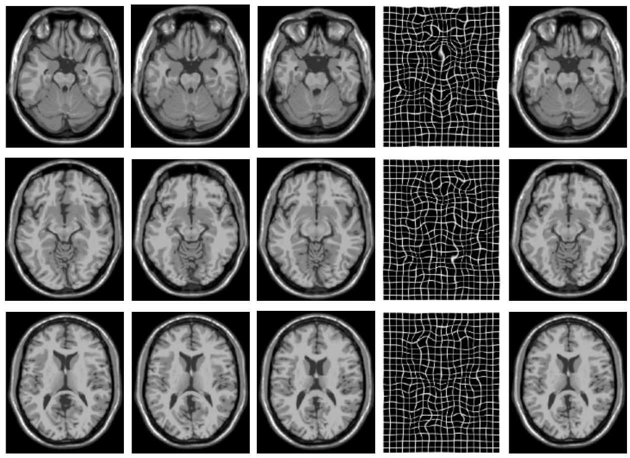

Figure 4: Synthetic experiments without noise. From top to bottom, the rows correspond to reference slices 49, 61 and 86, respectively. From left to right, the first column shows the floating (deformable)images; the second column shows the registration result after the Diff demons; the third column shows the registration result after the proposed; the fourth column shows the deformation grids after the proposed; the fifth column shows the reference images

We conduct synthetic experiments on 2-D T1-weighted MR images($217 \times 181$ pixels each image) from the BrainWeb database. Three pairs of slices are selected randomly from the 2-D T1-weighted mode sequences in the database, each pair consists of a reference slice from normal brain database and a floating slice which come from MS lesions database. They are

Table 1: Error (%)) On The Brainweb Database Without Noise

| Reference Slice | m | Proposed Method | | | | | | | | | | Diff Demons |
|---|---|---|---|---|---|---|---|---|---|---|---|---|
| | | k=110 | 120 | 130 | 140 | 150 | 160 | 170 | 180 | 190 | 200 | |
| 49 | 133 | 8.59 | 8.03 | 6.91 | 6.52 | 7.87 | 10.07 | 9.97 | 10.01 | 11.53 | 10.98 | 6.49 |
| | 123 | 8.24 | 7.49 | 6.34 | 6.81 | 6.45 | 8,51 | 8.78 | 9.59 | 10.02 | 10.14 | |
| | 113 | 9.92 | 8.54 | 6.68 | 7.87 | 7.53 | 8.49 | 9.12 | 9.31 | 9.54 | 9.86 | |
| 61 | 133 | 9.27 | 8.09 | 7.34 | 7.17 | 6.9 | 7.98 | 8.99 | 6.54 | 8.52 | 8.89 | 6.63 |
| | 123 | 10.61 | 9.86 | 8.09 | 7.89 | 8.13 | 8.57 | 7.69 | 6.44 | 7.99 | 9.63 | |
| | 113 | 10.27 | 9.46 | 9.16 | 9.21 | 8.57 | 7.39 | 7.02 | 7.21 | 7.97 | 8.92 | |
| 86 | 133 | 8.18 | 7.67 | 6.62 | 8.53 | 6.99 | 8.82 | 8.34 | 10.12 | 9.58 | 9.83 | 6.54 |
| | 123 | 7.62 | 6.51 | 8.39 | 9.17 | 9.68 | 9.43 | 9.98 | 10.12 | 9.78 | 9.67 | |
| | 113 | 8.92 | 6.33 | 7.87 | 8.07 | 7.78 | 8.65 | 9.42 | 9.85 | 9.76 | 9.81 | |

Table 2: Error (%)) On The Brainweb Database With Noise

| Reference Slice | m | Proposed Method | | | | | | | | | | Diff Demons |
|---|---|---|---|---|---|---|---|---|---|---|---|---|
| | | k=210 | 220 | 230 | 240 | 250 | 260 | 270 | 280 | 290 | 300 | |
| 49 | 133 | 8.76 | 8.47 | 7.21 | 7.37 | 8.59 | 9.97 | 10.17 | 9.81 | 10.59 | 11.12 | 7.59 |
| | 123 | 8.94 | 7.99 | 7.19 | 7.49 | 8.51 | 9.17 | 9.98 | 9.65 | 10.08 | 10.78 | |
| | 113 | 10.92 | 9.64 | 8.58 | 7.57 | 8.55 | 9.23 | 10.22 | 9.89 | 10.18 | 10.25 | |
| 61 | 133 | 11.03 | 10.89 | 10.35 | 9.97 | 8.68 | 9.03 | 8.49 | 7.52 | 8.33 | 9.27 | 7.85 |
| | 123 | 10.14 | 9.92 | 10.07 | 9.81 | 8.65 | 8.99 | 7.43 | 7.09 | 7.5 | 9.63 | |
| | 113 | 11.45 | 9.76 | 10.32 | 9.34 | 9.98 | 9.57 | 7.32 | 6.97 | 7.8 | 9.39 | |
| 86 | 133 | 8.69 | 7.45 | 8.34 | 9.55 | 9.58 | 9.69 | 9.82 | 10.16 | 10.07 | 10.69 | 7.43 |
| | 123 | 8.89 | 7.38 | 9.07 | 9.37 | 9.48 | 9.89 | 10.21 | 10.57 | 9.91 | 10.22 | |
| | 113 | 9.17 | 7.27 | 7.47 | 8.07 | 9.09 | 9.35 | 10.23 | 10.39 | 10.97 | 10.08 | |

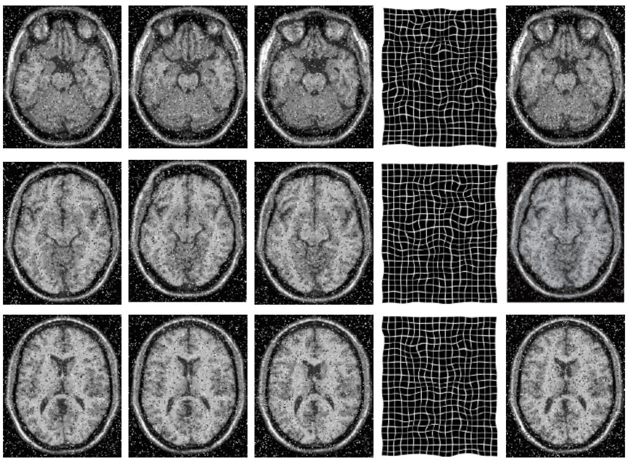

Figure 5: Synthetic experiments with noise. From top to bottom, the rows correspond to reference slices 49, 61 and 86, respectively. From left to right, the first column shows the floating (deformable) images; the second column shows the registration result after the Diff demons; the third column shows the registration result after the proposed; the fourth column shows the deformation grids after the proposed; the fifth column shows the reference images

further separated into two groups, one with 3% noises, the other without noises.

Table I and Table II show errors on the BrainWeb database without noise and with noise, respectively. We randomly select reference slices 49, 61 and 86 from the normal brain database as reference images and the correspondent floating slices 52, 59 and 88 from MS lesion brain database. For the noiseless setting, the choice of neiborghood is empirically from $k_{min} = 100$ to $k_{max} = 200$. As shown in Table I, the proposed adaptive method for SPD matrices on Lie group achieves superior performances in most tests. Though possibly a larger error in some tests, there must exist at least one item, for which the proposed could obtain a lower error. In the case of slice 49, the error on 123-dimension with $k = 130$ is 6.34%, which is much lower than the result 10.12 with $k = 190$, and lower than 6.49% of the Diff Demons, while in the case of slices 61 and 86, we obtain the best results of 6.44% for $m = 123, k = 180$ and 6.33% for $m = 113, k = 120$, respectively. It indicates that a larger neighborhood is needed for slice 61 to approximation to the local tangent space than slices 49 and 86.

In Table II, we add 3% noise to achieve more realistic results, our algorithm needs a relatively larger neighborhood to identify the local tangent space, parameter $k$ ranges from 200 to 300. Compared with the Diff Demons method, our method in the noisy setting demonstrates more remarkable advantage than that in the noiseless setting. Without noise, the new method yields lower error than control in 6 of the cases. The number increases to 14 when noise presents, the main reason is that adaptive selection of neighborhood using PCA can reduce the noise [27]. We preserve 95% of data energy in PCA processing.

In Fig.4 and Fig.5, from top to bottom, the first row corresponds to slice 49 with $m = 123$ and $k = 130$ or $m = 123$ and $k = 230$, the second row corresponds to slice 61 with $m = 123$ and $k = 180$ or $m = 123$ and $k = 280$; the third row corresponds to slice 86 with $m = 113$ and $k = 120$ or $m = 113$ and $k = 220$. From left to right, the first column shows the floating(deformable)images; the second column shows the registration result after the Diff demons method, the third column shows the registration result after the proposed adaptive method; the fourth column shows smooth deformation grids, the proposed adaptive produce topology preservation without any overlap and tear, the fifth column shows the reference images. One can clearly observe that more similarity exists between the third column (the result after the proposed) and the fifth column (the reference images) than that between the second column (the result after the Diff Demons) and the fifth column.

In Fig.6, slice 49 with and without noise are sampled for comparison of the degree of topology preservation $d_{TP}$. More iterations are required for the proposed algorithm to converge to the final solution, but higher degree is obtained. Our algorithm is sensitive to the size of neighborhood, as well as the varied dimension. Comparison of noiseless results are depicted in (a), (c) and (e), respectively. According to the data in Table I, we set parameter $k = \{120, 130, 140\}$. The $d_{TP}$ reported in Diff Demons is 90%, two results in our approach exceed 90%, the best one achieves 91.2% with $k = 130$ and $m = 123$ shown in (c), another one is 90.6% with $k = 120$ and $m = 133$ shown in (e). (b), (d) and (f) describe comparison of noisy results, here $k = \{230, 240, 250\}$, The $d_{TP}$ with Diff Demos is 84%. In our proposed approach, three results exceed 84%, the maximal value of $d_{TP}$ is 86%.

#### 4.3.3 Clinical Data

As shown in Fig.7 and 8, clinical data consist of four groups: the gray matter without and with noise, the white matter without and with noise. In the gray matter data without and with noise, the best performance appear when $m = 113, k = 120$ and $m = 113, k = 240$, respectively. In the white matter data without and with noise,the best results are reported with $m = 123, k = 160$ and $m = 123, k = 270$.

Fig.9 indicates comparison of the convergence on Diff Demons and the proposed. Due to the mapping between high dimension tangent space and the Lie group, the proposed method needs more iterations to reach convergence. However, as shown in Fig.9 (a)-(d), the proposed algorithm produces convergence till the 60th iteration, RMS errors in noiseless setting (a) and (b) are not higher than the result of Diff Demons from the 60th iteration and begin to converge, RMS errors in noisy setting (c) and (d) become lower than the result of Diff Demons from the 60th iteration and begin to converge.

## 5 Conclusions And Future Work

In this paper, we present a novel approach for topology-preserving deformable registration in medical images. Our work is devoted to enforce topology preservation by using adaptive neighborhood selection to approximate tangent space. We consider the structure of data and the influence of noise which are ignored in the previous methods. The proposed method adopts the Lie group structure of symmetric positive definite matrices with dense and high dimensional features. Furthermore, our results show the sensitivity of our proposed algorithm to the different dimension and neighborhood size of the transformed SPD. Compared with the original method, experiment results indicate a higher accuracy, particularly, these results in the presence of noisy.

In future, we will focus on two problems. First, due to iteratively mapping to the high dimensional tangent spaces, the algorithm power is obtained at the expense of computational efficiency; second, though there always exists a configuration from the size of neighborhood and the size of dimension reaching expected performance, it is still not theoretically clear how to select the configuration following some certain rule. If we can find the rule so as to ensure configurations from the possible set without enumeration, the amount of work in experiments can be reduced. However, determining the intrinsic dimensionality of data is a difficult issue. We will address these problems in the future work.

**Acknowledgements:** This research is supported by the Sheng-Bu Industry-Academia-Research joint project of Education Ministry and Science & Technology Ministry of Guangdong province (NO: 2012A090300001).

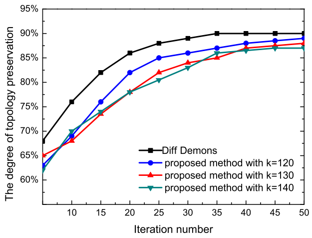


(a) m=113 without noise

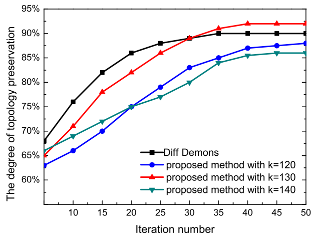


(b) m=123 without noise

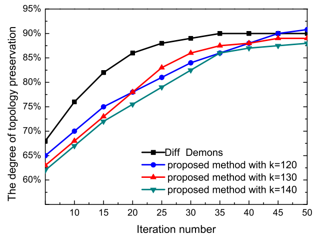


(c) m=133 without noise

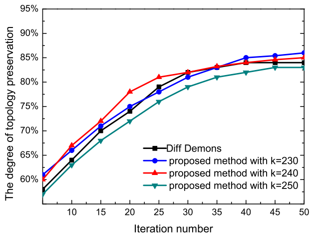


(d) m=113 with noise

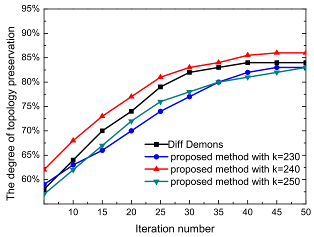


(e) m=123 with noise

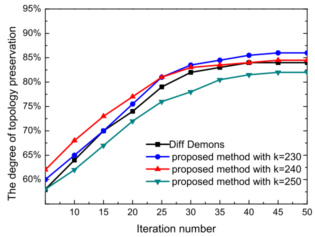


(f) m=133 with noise

Figure 6: Comparison of the degree of topology preservation: (a)(c)(e) in the noiseless setting; (b)(d)(f) in the noisy setting

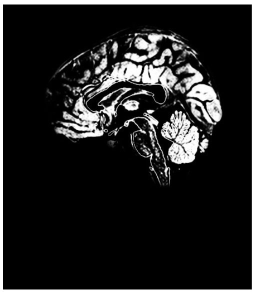

(a)

(b)

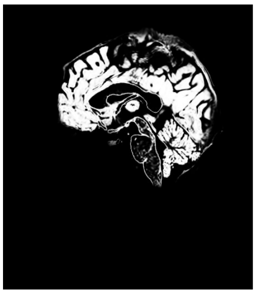

(c)

(d)

(e)

(f)

(g)

(h)

Figure 7: Clinical data without noise. The first row shows grey matter images, the second row shows white matter images. (a)(e) reference images; (b)(f) floating images; (c)(g) the results after 30 iterations; (d)(h) the results after 60 iterations

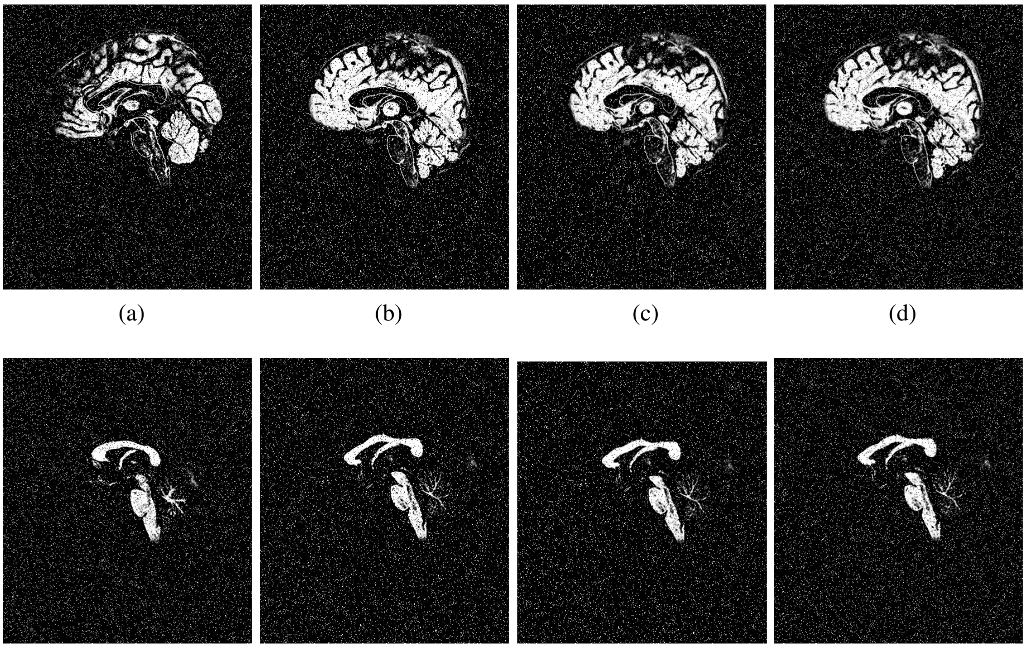

(a) (b) (c) (d)

(e) (f) (g) (h)

Figure 8: Clinical data with noise. The first row shows grey matter images, the second row shows white matter images. (a)(e) reference images; (b)(f) floating images; (c)(g) the results after 30 iterations; (d)(h) the results after 60 iterations

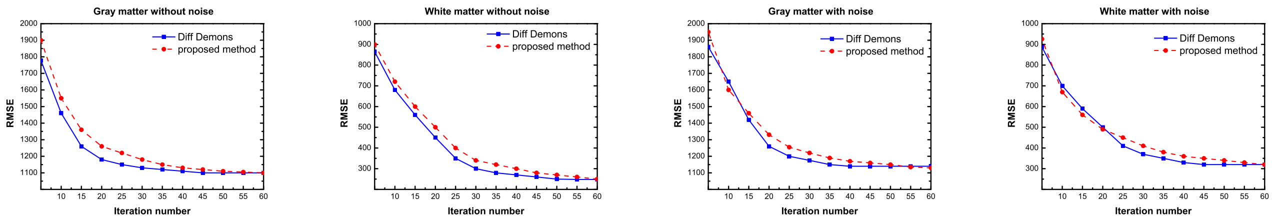


(a) (b) (c) (d)

Figure 9: Comparison of RMS error on clinical data

*References:*

[1] Z. Kerekes, Z. Toth, S. Szenasi, Z. Vamossy and Sz. Sergyan, “Colon cancer diagnosis on digital tissue images,” *Proceedings of IEEE 9th International Conference on Computational Cybernetics Tihany, 2013*, pp. 159-163.

[2] S. Sznsi, “Segmentation of colon tissue sample images using multiple graphics accelerators,” *Computers in Biology and Medicine* , Vol. 51, pp. 93-103, 2014.

[3] O. Musse, F. Heitz, and J. P. Armspach, “Topology preserving deformable image matching using constrained hierarchical parametric models,” *Image Processing, IEEE Transactions on*, vol. 10, no. 7, pp. 1081–1093, 2001.

[4] V. Noblet, C. Heinrich, F. Heitz, and J.-P. Armspach, “3-d deformable image registration: a topology preservation scheme based on hierarchical deformation models and interval analysis optimization,” *Image Processing, IEEE Transactions on*, vol. 14, no. 5, pp. 553–566, 2005.

[5] T. Rohlfing, C. R. Maurer Jr, D. Bluemke, M. Jacobs *et al.*, “Volume-preserving nonrigid registration of mr breast images using free-form deformation with an incompressibility constraint,” *Medical Imaging, IEEE Transactions on*, vol. 22, no. 6, pp. 730–741, 2003.

[6] G. E. Christensen, R. D. Rabbitt, M. Miller *et al.*, “Deformable templates using large deformation kinematics,” *Image Processing, IEEE Transactions on*, vol. 5, no. 10, pp. 1435–1447, 1996.

[7] G. E. Christensen, M. Miller, M. W. Vannier, U. Grenander *et al.*, "Individualizing neuroanatomical atlases using a massively parallel computer," *Computer*, vol. 29, no. 1, pp. 32–38, 1996.

[8] B. Karaçali and C. Davatzikos, "Estimating topology preserving and smooth displacement fields," *Medical Imaging, IEEE Transactions on*, vol. 23, no. 7, pp. 868–880, 2004.

[9] J. Ashburner, J. L. Andersson, and K. J. Friston, "High-dimensional image registration using symmetric priors," *NeuroImage*, vol. 9, no. 6, pp. 619–628, 1999.

[10] E. Haber and J. Modersitzki, "Image registration with guaranteed displacement regularity," *International Journal of Computer Vision*, vol. 71, no. 3, pp. 361–372, 2007.

[11] S. Marsland and C. J. Twining, "Constructing diffeomorphic representations for the groupwise analysis of nonrigid registrations of medical images," *Medical Imaging, IEEE Transactions on*, vol. 23, no. 8, pp. 1006–1020, 2004.

[12] J. Ashburner, "A fast diffeomorphic image registration algorithm," *Neuroimage*, vol. 38, no. 1, pp. 95–113, 2007.

[13] V. Arsigny, O. Commowick, X. Pennec, and N. Ayache, "A log-euclidean framework for statistics on diffeomorphisms," *Medical Image Computing and Computer-Assisted Intervention–MICCAI 2006*. Springer, 2006, pp. 924–931.

[14] T. Vercauteren, X. Pennec, A. Perchant, and N. Ayache, "Diffeomorphic demons: Efficient non-parametric image registration," *NeuroImage*, vol. 45, no. 1, pp. S61–S72, 2009.

[15] V. Arsigny, "Processing data in lie groups: an algebraic approach. application to non-linear registration and diffusion tensor mri," Ph.D. dissertation, Ecole Polytechnique X, 2006.

[16] Z. Zhang, J. Wang, and H. Zha, "Adaptive manifold learning," *Pattern Analysis and Machine Intelligence, IEEE Transactions on*, vol. 34, no. 2, pp. 253–265, 2012.

[17] S. T. Roweis and L. K. Saul, "Nonlinear dimensionality reduction by locally linear embedding," *Science*, vol. 290, no. 5500, pp. 2323–2326, 2000.

[18] J. B. Tenenbaum, V. De Silva, and J. C. Langford, "A global geometric framework for nonlinear dimensionality reduction," *Science*, vol. 290, no. 5500, pp. 2319–2323, 2000.

[19] R. Mahony and J. H. Manton, "The geometry of the newton method on non-compact lie groups," *Journal of Global Optimization*, vol. 23, no. 3-4, pp. 309–327, 2002.

[20] V. Arsigny, P. Fillard, X. Pennec, and N. Ayache, "Geometric means in a novel vector space structure on symmetric positive-definite matrices," *SIAM journal on matrix analysis and applications*, vol. 29, no. 1, pp. 328–347, 2007.

[21] O. Tuzel, F. Porikli, and P. Meer, "Region covariance: A fast descriptor for detection and classification," in *Computer Vision–ECCV 2006*. Springer, 2006, pp. 589–600.

[22] R. Caseiro, P. Martins, J. F. Henriques, and J. Batista, "A nonparametric riemannian framework on tensor field with application to foreground segmentation," *Pattern Recognition*, vol. 45, no. 11, pp. 3997–4017, 2012.

[23] X. Lin, T. Qiu, F. Morain-Nicolier, and S. Ruan, "A topology preserving non-rigid registration algorithm with integration shape knowledge to segment brain subcortical structures from mri images," *Pattern Recognition*, vol. 43, no. 7, pp. 2418–2427, 2010.

[24] Z. Zhang and H. Zha, "Principal manifolds and nonlinear dimension reduction via local tangent space alignement," *Department of computer science and engineering, Pennsylvania State University, Tech. Rep. CSE-02-019*, 2002.

[25] J. Carreira, R. Caseiro, J. Batista, and C. Sminchisescu, "Semantic segmentation with second-order pooling," in *Computer Vision–ECCV 2012*. Springer, 2012, pp. 430–443.

[26] C. Xu, C. Lu, J. Gao, W. Zheng, T. Wang, and S. Yan, "Discriminative analysis for symmetric positive definite matrices on lie groups."

[27] P. N. Belhumeur, J. P. Hespanha, and D. J. Kriegman, "Eigenfaces vs. fisherfaces: Recognition using class specific linear projection," *Pattern Analysis and Machine Intelligence, IEEE Transactions on*, vol. 19, no. 7, pp. 711–720, 1997.